

# The effects of photobiomodulation and low-amplitude high-frequency vibration on bone healing process: a comparative study

M. Rajaei Jafarabadi<sup>1</sup> · G. Rouhi<sup>2</sup> · G. Kaka<sup>3</sup> · S. H. Sadraie<sup>4</sup> · J. Arum<sup>3</sup>

Received: 15 April 2016 / Accepted: 17 August 2016 / Published online: 30 August 2016  
© Springer-Verlag London 2016

**Abstract** This study aimed at investigating the effects of photobiomodulation (PBM) and low-amplitude high-frequency (LAHF) whole body mechanical vibration on bone fracture healing process when metallic plates are implanted in rats' femurs. Forty male rats weighing between 250 and 350 g, 12 weeks old, were employed in this study. A transverse critical size defect (CSD) was made in their right femurs that were fixed by stainless steel plates. After the surgery, the rats were divided equally into four groups: low-level laser therapy group (GaAlAs laser, 830 nm, 40 mW, 4 J/cm<sup>2</sup>, 0.35 cm beam diameter, LLLT), whole body vibration group (60 Hz, 0.1 mm amplitude, 1.5 g, WBV), a combination of laser and vibration group (LV), and the control group (C). Each group was divided into two subgroups based on sacrifice dates. The rats were sacrificed at intervals of 3 and 6 weeks after the surgery to extract their right femurs for radiography and biomechanical and histological analyses, and the results were analyzed using standard statistical methods. Radiographic analyses showed greater callus formation in the LLLT and WBV groups than in control group at both 3 ( $P < 0.05$  and  $P < 0.001$ , respectively) and 6 weeks after surgery ( $P < 0.05$  and  $P < 0.05$ , respectively). Histological evaluations showed a higher amount of new bone formation and better maturity in the LLLT and

WBV groups than the control groups at 3 and 6 weeks after surgery. Biomechanical tests showed that the maximum force at fracture in the LLLT ( $P < 0.05$  in 3 weeks and  $P < 0.05$  in 6 weeks) and WBV ( $P < 0.001$  in 3 weeks and  $P < 0.05$  in 6 weeks) groups was greater than that in the control groups at both time intervals. But a combination of laser and vibration therapy, LV, did not show a positive interaction on bone fracture healing process. The biostimulation effects of PBM or LLLT and of low-amplitude high-frequency WBV both had a positive impact on bone healing process, for critical size defects in the presence of a stainless steel implant. But their combination, i.e., low-level laser therapy and low-amplitude high-frequency whole body vibration (LV), interestingly did not accelerate the fractured bone healing process.

**Keywords** Bone fracture healing · Mechanobiology · Photobiomodulation · Low-level laser therapy · Low-amplitude high-frequency whole body vibration · Critical size defects · Stainless steel implant · Animal tests

## Introduction

When a bone is fractured, the time required for the full recovery can be too long, which can have a negative socioeconomical impact on the society. Bone defects can appear either by necrosis, or pathological conditions, or surgeries, and/or trauma. These defects may be larger compared to those that can heal quickly without medical/surgical intervention. In these circumstances, medical and/or surgical methods, for instance, can be employed to help heal bone faster. In order to accelerate the bone healing process and osteogenesis stimulation, various methods were introduced and practiced to date. These methods include but not limited to hormone injection, vitamin and mineral intake, local blood

✉ G. Rouhi  
grouhi@uottawa.ca

<sup>1</sup> Materials and Biomaterials Research Center (MBMRC), Tehran, Iran

<sup>2</sup> Faculty of Biomedical Engineering, Amirkabir University of Technology, Tehran, Iran

<sup>3</sup> Neuroscience Research Center, Baqiyatallah University of Medical Sciences, Tehran, Iran

<sup>4</sup> Department of Anatomy, Baqiyatallah University of Medical Sciences, Tehran, Iran

supply increase, application of mechanical load, use of ultrasound and/or electrical stimulation, and recently application of low-level laser therapy [1–3]. Studies showed that the aforementioned methods encourage bone formation, increase bone mass, and accelerate the fracture healing process [4, 5]. Some studies in the field of bone healing tried to compare the effectiveness of various methods of accelerating bone healing process, and also delve into creation of some kind of interaction among various methods [1, 6–9]. One method that is often recommended in order to decrease the bone fracture healing time is photobiomodulation [10–13]. Photobiomodulation or low-level laser therapy (LLLT) is a drug-free, noninvasive, and safe clinical application of light, usually produced by low- to mid-power lasers or light emitting diodes (LED), with a power output in the range of 1–500 mW to a patient to promote tissue regeneration and healing, reduce inflammation, and relieve pain. The light is in the visible (red) or near infrared (NIR) spectrum (600–1000 nm) and achieves an average power density between 1 and 5 W/cm<sup>2</sup> [14]. Despite the fact that effectiveness of LLLT on bone fracture healing is not yet universally accepted, nonetheless, there were a lot of promising results in regard to the impact of LLLT in recent experimental studies [5, 15, 16]. In recent years, the optimal intensity of laser and the effect of LLLT on bone-implant interface were also noticed [17]. Moreover, it is difficult to compare the results of various studies involving low-level laser therapy treatment existing in the literature, because of the diversity of techniques, method of experiment and experimental models employed, as well as the limitations of the reported treatment protocols [18].

Pinheiro et al. suggested laser intensities between 1.8 and 5.4 J/cm<sup>2</sup> suitable for laser therapy [10]. Nissan et al. compared two laser intensities of 4 and 10 J/cm<sup>2</sup> in animal models and concluded that 4 J/cm<sup>2</sup> intensity has better effects on the accumulation of radio calcium in less time [19]. Their results suggested that continuous laser had more advantages than pulsed laser, and very low or high intensity lasers were ineffective, or even have negative effects [5]. Hence, scientists now use continuous lasers with 4 J/cm<sup>2</sup> intensity [20]. In an experimental study on rabbit's tibia, Khadra et al. found that laser therapy (GaAlAs, 830 nm, 150 mW) accelerated the bone fracture healing process and had a positive impact on bone-titanium implant interface compared to the control group [17]. Pereira et al. in a histomorphometric study on bone-titanium implant interface quality showed that despite the fact that there was no difference between newly bone formed in the laser therapy and control groups, the quality of contact between the implant and bone was better in the laser group [21]. Maluf et al. studied mechanical effects of laser therapy on implants [22]. In their study, a screw-shaped titanium implant was placed in rat's femur, and after 2 weeks of laser therapy, it was pulled out by a torque meter. The amount of torque necessary to pull off the screws of the rat's femur in the

laser group was about 50 % more than in the control group [5]. Eventually, Diniz et al. reported that laser therapy (GaAlAs, 4 J/cm<sup>2</sup>) on bone, without the implant, has no effects on the bone healing process [8].

Among numerous factors influencing bone healing and remodeling, functional mechanical loading from whole body vibration may be sensed by bone cells as a potent extrinsic signal [23, 24]. Whole body vibration not only includes large forces generated by vigorous physical activities, such as running or weightlifting, but it also includes very small-magnitude forces associated with subtle events such as posture [23]. When these low-level mechanical signals are delivered at sufficiently high frequencies, such as by standing on a vertically oscillating plate, they can stimulate bone cells to enhance bone formation, decrease resorption, and remodel bone into a stiffer and stronger structure with improved architectural characteristics [25–29]. Application of these extremely low-magnitude high-frequency mechanical stimuli in recent human studies suggested beneficial effects in a healthy skeleton and in skeletons disturbed by local or systemic stimuli, including inactivity, hormonal changes, or low bone mass [30–32]. The physical mechanisms by which cells can perceive a very small signal caused by low-magnitude high-frequency mechanical vibration have not been identified yet [33]. The efficacy of the much larger exercise-induced mechanical signals has been related to the magnitude of the generated tissue deformation [34]. Matrix deformation does not appear necessary for high-frequency, low-level mechanical stimuli to influence cell activity [35]. High-frequency oscillatory accelerations applied as unconstrained motions may serve as a regulatory physical signal to increase bone formation in a healthy bone [24], as well as prevent bone loss [36] and improve mechanical properties during disuse [37]. Oscillatory accelerations, rather than deformations, can be easily applied to any skeletal segment, either weight bearing or not. Even though the clinical advantages of a stimulus that is barely detectable and involves motions on the order of only 100  $\mu$ m are apparent, however, whether or not such a stimulus can enhance osteogenesis in a bone defect is not yet fully known [38].

Based on the anabolic effects of both LLLT and low-amplitude high-frequency (LAHF) whole body vibration on bone, it is hypothesized here that the association of these two methods of therapy, i.e. LLLT + LAHF, can further accelerate the bone fracture healing process. Thus, in this study, the effects of low-level GaAlAs (830 nm) laser therapy, as well as low-amplitude high-frequency whole body vibration, and a combination of these two methods on bone fracture healing process, in the presence of a stainless steel plate implanted in a critical size defect (CSD) of the rats' femurs, were investigated.

## Materials and methods

Forty male, 12 weeks old, Wistar rats weighting between 250 and 350 g (Baqiyatallah Medical University, Tehran, Iran) were used to investigate the effects of LLLT and LAHF whole body vibration on healing of transected fracture of their femurs. The rats were housed two per cage in  $60 \times 40 \times 40 \text{ cm}^3$  ( $L \times W \times H$ ) acrylic glass cages in a temperature-controlled room with a 12:12-h light-dark cycle, which were provided standard rodent chow and water ad libitum. Animals were transferred to these cages 1 week prior to the experiment date in order to acclimate them to their new environment. Animals were randomly divided into four groups (10 rats per group): (1) low-level laser therapy group (LLLТ), (2) low-amplitude high-frequency whole body vibration group (WBV), (3) combination of laser and whole body vibration group (LV), and (4) control group (CG).

The animals were anesthetized with a mixture of 90 mg/kg ketamine hydrochloride and 8 mg/kg xylazine hydrochloride intraperitoneally [39]. The skin on the lateral face of the right thigh of each rat was shaved and disinfected with 1 % of antiseptic povidone-iodine [40], and all surgical procedures were carried out under sterile conditions. The animals were then positioned in ventral decubitus, and the front and hind paws were fixed in an abducted position. The incision location was then prepared with antiseptic (iodide alcohol), and a direct incision to access the femur bone was made with a scalpel. Following incision and femur exposure, four 0.8-mm diameter holes were drilled on the femur based on the pattern of the implant's holes, then the stainless steel plate ( $20 \times 4 \times 1 \text{ mm}^3$ ) was mounted on diaphysis and fixed. After fixing the implant on the rat's femur with orthodontical wires (0.7 mm diameter), a transverse cut was created on the cranialateral face of the femur at approximately 20 mm distance from the proximal epiphysis of the femur. The critical size defect was made with a specific blade with a 300- $\mu\text{m}$  thickness, mounted on a saw (see Fig. 1). The incision was sterilized and sutured immediately and animals were transferred to their cages.

### Low-amplitude high-frequency whole body vibration

The vibration system consisted of a custom-made vibration platform attached to two stepper motors and two cams, which delivered vertical vibrations, and the waveform and frequency of the vibration provided by the motors were controlled with a PLC [26]. Vibration amplitude was restrained by four lock screws and springs in each corner of the platform, and some lead blocks which were attached under the platform can stabilize and regulate the vibration. The specifications of the vibrator were set on regular vibration regime with a 0.1-mm amplitude, frequency of 60 Hz, and acceleration of 1.5 g, and

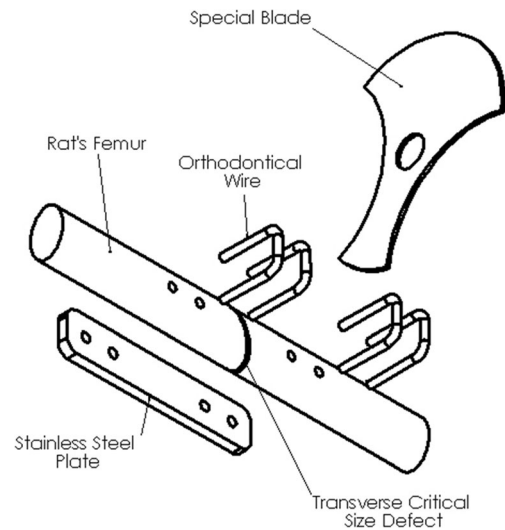


**Fig. 1** Schematic depiction of the rat femur and the internal fixator's components. Critical size defect was made by a special blade and stainless steel plate and was fixed by orthodontical wires

the vibration was applied on the rats for 5 days a week and 20 min per day [27].

### Low-level laser therapy

A low-energy GaAlAs (PMS1252, INLC, Tehran, Iran), 830 nm, CW, 0.35 cm beam diameter, 40 mW, energy of 1.52 J at 4 J/cm<sup>2</sup> with irradiation time of 38 s were used in this study. Laser irradiation was initiated immediately after the surgery and was performed every 48 h postsurgery. Laser irradiation was performed transcutaneously at one point right above the site of injury, using the punctual contact technique. After 21 and 42 days postsurgery, animals were exposed to a total dose of 36 and 72 J/cm<sup>2</sup> of laser radiation, respectively. After two intervals of 3 and 6 weeks, the rats were sacrificed by overdose of anesthesia and their right femurs were disarticulated from the hip and trimmed to remove excess muscle, skin, and other soft tissues.

### Scoring for callus formation

All bone specimens were examined by X-ray imaging (Senographe 600T Senix HF) and assessed semiquantitatively, on a graded scale and based on a modified criterion for scoring by Madsen and Hukkhanen [41] (Table 1). The specimens were evaluated twice in a blinded fashion with respect to treatment modality by an experienced pathologist, and each score was checked randomly by another pathologist. When there was a disagreement between the investigators, a consensus was reached for that section.

**Table 1** Callus formation scoring based on the method of Madsen and Hukkhanen [41]

| Callus formation |                      |
|------------------|----------------------|
| Score 0          | No callus formation  |
| Score 1          | Very minimal callus  |
| Score 2          | Minimal callus       |
| Score 3          | Normal callus        |
| Score 4          | Low excessive callus |
| Score 5          | Excessive callus     |

### Biomechanical analysis

Biomechanical properties of the right femurs were determined by a three-point bending test with a 5-kN load. The proximal and distal aspects of each femur were then placed in the grips of a hydraulic material testing machine, Zwick System, Germany, with a 2.0-cm distance between two grips. The load cell was perpendicularly positioned in the posterior-anterior direction at the exact site of the bone defect. A 5-N preload was applied in order to avoid specimen sliding. Finally, the bending force was applied at a constant deformation rate of 5 mm/min until fracture occurred [42]. From the load-deformation curve, the maximum load at failure (in N) was determined.

### Histological and statistical analyses

After X-ray imaging and biomechanical tests, the specimens were stored in a 10 % neutral buffered formalin for 2 days and then decalcified in 10 % nitric acid solvent [43]. The specimens were processed in a Citadel 2000 tissue processor (Shandon, UK) and embedded in paraffin wax. Five micrometer thickness from paraffin-embedded tissue was serially sectioned longitudinally and stained with a standard hematoxylin and eosin stain for histological evaluation. Histological evaluation was performed by a pathologist, who was blinded to the treatment, under a light microscope (magnification of  $\times 400$ ). In addition, histological analyses were performed using the Osteometrics software to determine the area of bone, cartilage, and connective vascular tissue (a subtraction of bone and cartilage callus tissues from total area) formation by manual tracing. Pre-existing cortical bone was excluded from the histological analysis. The total area for each sample was then used to quantify the percentage areas of bone, cartilage, and connective vascular tissue. At least five nonconsecutive sections were used for histological analyses. A minimum of 15 samples were included in each group, and the mean of areas of these 15 samples was used in statistical analysis to determine the composition of the fracture callus. The nonparametric Tukey test was then used to compare data for the four experimental groups and two

periods of study, i.e., 21 and 42 days, and the differences were considered significant for  $P \leq 0.05$ .

## Results

### Radiographic images

Radiologic definition of the bone defect area and the callus formation were observed in all groups. On day 21 after surgery, satisfactory radiopacity of the defect area was noted in the control group, as well as radiolucent areas in the other experimental groups (Fig. 2, upper row). On day 42 after surgery, in the groups receiving laser, vibration, and laser and vibration (LLLT, WBV, and LV), there was a well-defined radiopaque contour of the border of the bone defect, indicating new bone and hard callus formations (Fig. 2, lower row).

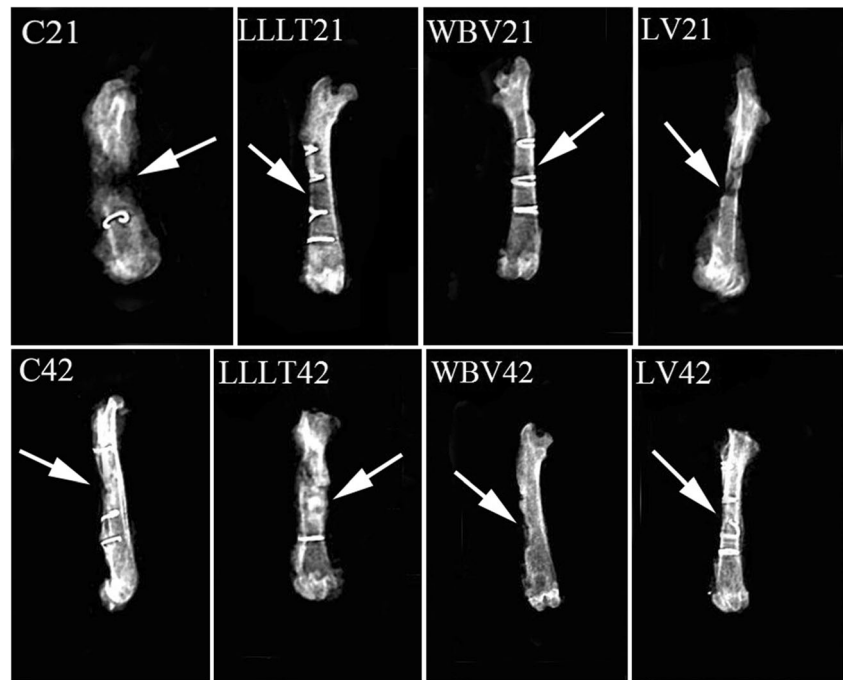
The radiographic images obtained showed a pattern of callus formation and bone growth from the edges of the critical size defect was irregular in their distribution (Fig. 2). In relation to the effects of various treatments among different groups, there was a significant difference between the laser and vibration groups in 3 ( $P < 0.05$  and  $P < 0.001$ , respectively) and 6 weeks, which can be seen in Fig. 3, of the closure of the CSD.

The semiquantitative scores of callus formation based on the method of Madsen and Hukkhanen [41] can be seen in Fig. 3. Scores of callus formation were divided into two different time periods, i.e., 21 and 42 days after surgery, for the control, laser, vibration, and laser + vibration groups. As can be seen, callus formation scores for the LLLT, WBV, and LV groups were greater than the control group (62.6, 73.3, and 62 %, respectively) on day 21 ( $P < 0.05$ ,  $P < 0.001$ , and  $P < 0.05$ , respectively), and this difference was decreased on 42 days compared to the control group on the same day (13, 4.3, and 6.6 %, respectively).

### Mechanical tests

The mechanical tests' results of the femur diaphysis can be seen in Fig. 4. The femur diaphysis was subjected to a three-point bending until it failed. On day 21 after surgery, in the LLLT, WBV, and LV groups, the treatments had a significant impact on the femur's maximum force at failure compared to the control group ( $P = 0.003$ ,  $P = 0.0003$ , and  $P = 0.001$ , respectively). Additionally, on day 42 after surgery, in the WBV and LV groups, a significant impact on maximum force at failure was observed ( $P = 0.004$  and  $P = 0.01$ , respectively), but in the LLLT group, there was no significant difference with the CG. In all treated groups, the maximum forces at failure were greater than in the control specimens. It is interesting to note that in all three groups, LLLT, WBV, and LV,

**Fig. 2** Radiographs obtained from the right femur of animals of groups C, LLLT, WBV, and LV on days 21 (*upper row*) and 42 (*lower row*) after surgery. Note the bone defect site (*white arrows*) containing the new bone formation that appears as a radiopaque image, and the radiolucent spaces show connective vascular tissues



compared to the control group (C21), the rate of healing for the first 3 weeks after the surgery was sharply increased but showed a much lower increase on day 42 after the surgery compared to C42.

### Histological analysis

After radiographic imaging and biomechanical tests, specimens were prepared for histological analyses, in which  $\times 400$  magnification images were captured. The surface area of bone trabeculae formation as well as the area of cartilage callus in histological images was calculated by a standard histological software (Motic Images 2000 (V1.2)). Then, by subtracting the sum of the two areas, belonging to bone and cartilage, from the total area, the connective vascular tissue (CVT) area was obtained. Figure 5 shows these areas at various time intervals for the four different groups under

investigation. Due to the large size of the defect, 21 days after surgery, the majority of the gap was filled with CVT and cartilage callus. As time went on, the area of CVT and cartilage callus was reduced and the bone trabeculae started to form. On day 21 postsurgery, the defects in C21 were filled by cartilage callus and a minor amount of woven bone tissue, with no interconnected trabeculae, was observed. These histological results confirmed the initial phase of bone repair. In the LLLT21, WBV21, and LV21 groups, animals demonstrated mild delimitation of the borders of the defect, and small amount of bone tissue, interconnected concentric trabeculae, and cartilage callus were observable, corresponding to a more advanced stage of bone repair, compared to the control group.

On day 42 postsurgery, the borders of the defect could still be observed in C42, with mild amount of newly formed bone surrounded by CVT. But in the LLLT42,

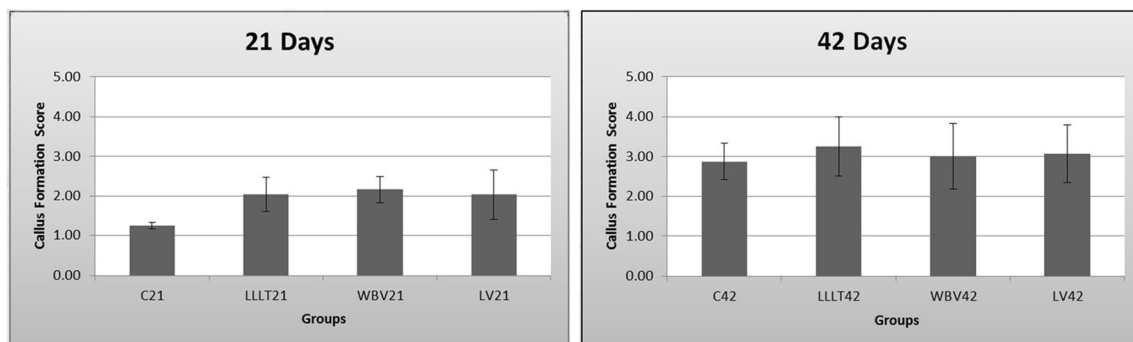
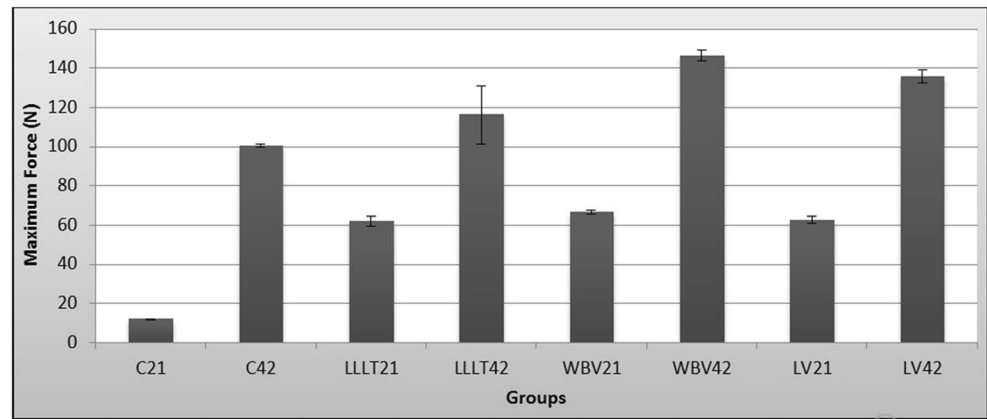


**Fig. 3** Callus formation scores for 21 and 42 days after surgery for different groups

**Fig. 4** Results of three-point bending tests on fractured femur for the four different groups, i.e., control (C), low-level laser therapy (LLLT), low-amplitude high-frequency whole body vibration (WBV), and a combination of laser and vibration (LV) on days 21 and 42 after surgery



WBV42, and LV42 groups, moderate amounts of new bone were produced, which represent a more advanced stage of bone healing compared to C42. In WBV42 and LV42, there was an intense presence of newly formed bone with interconnected trabeculae and organized tissue, with less area of cartilage callus, corresponding to a final stage of the bone healing process (Fig. 6).

Figure 7 shows the results of the histology tests. It can be observed that irradiated and vibrated animals, at the dosage and frequency used in this study, presented a higher amount of newly formed bone tissue compared to the control group. On day 21 postsurgery, the amount of new bone formation in the LLLT group is the highest among the other groups, but on day 42 postsurgery, the WBV group has the highest amount of new bone. In all the four groups under investigation, the amount of cartilage callus as well as CVT declined as time went on. Animals in the control group (C21 and C42) showed

significantly less bone formation compared to the animals in all the other groups ( $P < 0.05$ ).

## Discussion and conclusion

This work aimed at discovering the effects of LLLT, LAHF whole body vibration, and their combination (LLLT + WBV = LV) on rat's fractured femur, fixed with a metal plate, during the bone healing process. To the best of our knowledge, this study represents the first direct experimental investigation, using in vivo animal models, to compare the effects of LLLT and LAHF whole body vibration, as well as their combination, on the fractured bone healing process. Results of this study showed that all three treatment methods, i.e., LLLT, WBV, and LV, reduce bone fracture healing time; but surprisingly, the combinatorial application of LLLT and

**Fig. 5** Photomicrographs of the four groups under investigation 21 days after the surgery. Bone trabeculae (Tr), cartilage callus (C), and connective vascular tissue (CVT) can be seen in the different groups (C21, control group; LLLT21, laser-irradiated group; WBV21, vibrated group; LV21, laser-irradiated and vibrated group) on day 21 after surgery (hematoxylin and eosin staining,  $\times 400$  magnification)

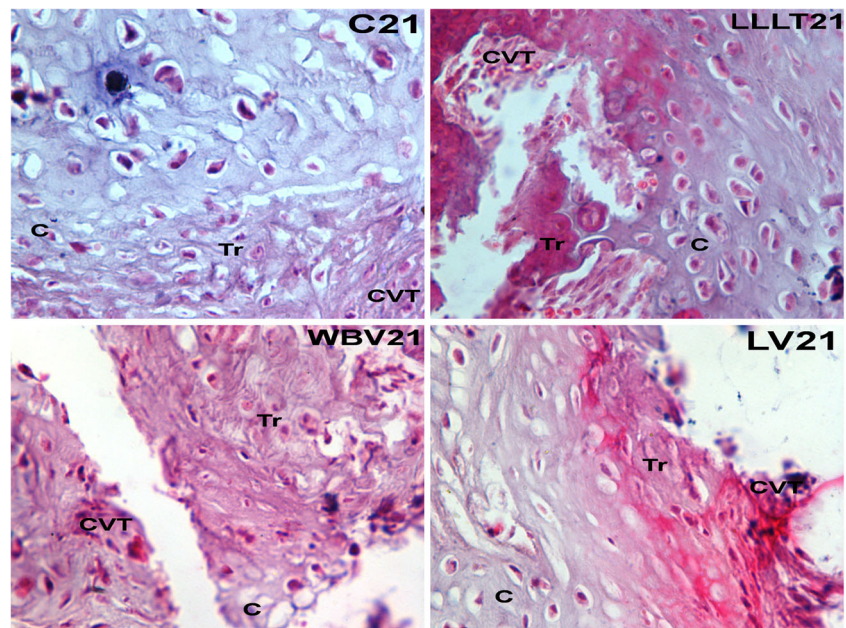
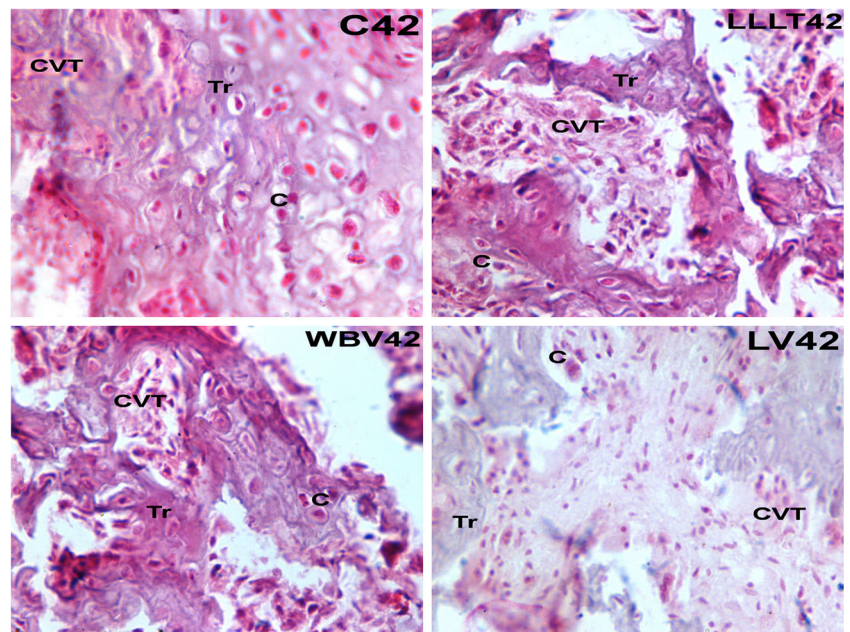


**Fig. 6** Photomicrographs of the four groups under investigation 42 days after the surgery. Bone trabeculae (*Tr*), cartilage callus (*C*), and connective vascular tissue (*CVT*) can be seen in the different groups (*C42*, control group; *LLLT42*, laser-irradiated group; *WBV42*, vibrated group; *LV42*, laser-irradiated and vibrated group) on day 42 after surgery (hematoxylin and eosin staining,  $\times 400$  magnification)



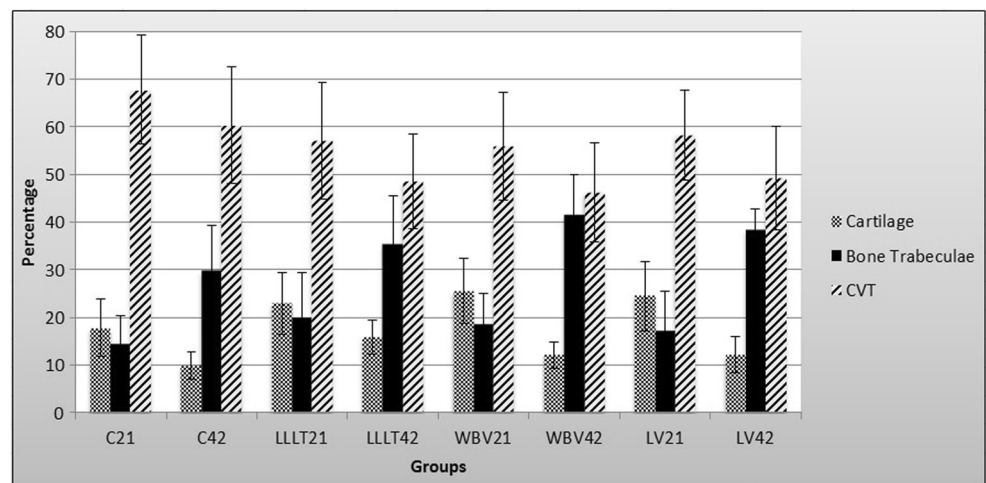
LAHF whole body vibration did not offer a more effective method compared to either method.

Three different types of tests were conducted in this study, i.e., radiographic imaging, biomechanical tests, and histologic imaging. Radiographs provide an accurate assessment of the structural anatomy of the skeleton and the position and alignment of the fracture fragments. They do not however differentiate between primary and secondary callus in the early stage of healing, nor do they provide any information about the mechanical status of the healing fracture. There was a strong change in optical density, compared to the control groups, represented by shades of gray in the laser-treated and whole body vibration groups of animals, as well as the presence of islets with higher optical density suggesting new bone formation (Fig. 2). The radiographic analyses suggested bone growth from the edge to the center of the defect, a well-

accepted point which was already reported by other researchers [44–47], confirming that there is a significant area of bone tissue formation versus the control group at week 6 after surgery. The result of X-ray imaging in this study suggested that there is a better callus formation in the LLLT and WBV groups compared to the control group (see Figs. 2 and 3). The comparison of X-ray images of LLLT21 and C21 suggested that LLLT affected the initial state of osteogenesis (Fig. 2), which is consistent with the findings reported in the literature [6, 48–51].

According to previous studies, LLLT accelerates the osteogenesis process in rats [11, 18, 52–56], especially when the fractured bones were fixed with metallic implants [5, 57, 58]. LLLT stimulates local cells which were exposed to laser radiation, but the LLLT effect cannot be observed at a long distance from the evaluated area [59–61]. Thus, in order to

**Fig. 7** Percentage of cartilage callus, bone trabeculae, and connective vascular tissues based on histological image analyses—images were analyzed by Motic images 2000, V1.2. Bars represent the 95 % confidence interval of five animals per group



regulate the osteogenesis process, the radiation zone must be controlled. On the other hand, there are many studies that investigated and approved the promising outcome of the effects of LAHF whole body vibration on the bone formation process [24, 28, 35, 36, 62]. The transmission of vibration to the body is a complex phenomenon because of nonlinearities of the human musculoskeletal system [63], LAHF whole body vibration applied indirectly on the fracture site, but the mechanical environment caused by vibration improved the load-bearing characteristics of bone (Fig. 4).

Comparing the mechanical and histological results of this study, it seems that despite the fact that the area of newly formed trabeculae bone in the LLLT group on day 21 after surgery is more than that of the WBV, the maximum force to failure corresponding to WBV is more than that of the LLLT group (see Figs. 4 and 5). The differences between the biomechanical properties of the two groups of laser and vibration treatments might indicate that even though the irradiated callus in the LLLT group has a larger volume, its mechanical properties are inferior to the WBV group. In other words, it seems that the callus in the irradiated group was more fibrocartilaginous and less ossified in nature on day 21 after surgery, while the callus in the vibrated group had already begun to ossify, a finding which is not in agreement with the results reported by Trelles and Mayoyo [64], Barushka et al. [65], and Luger et al. [5]. The use of critical size damage, which separated two ends of fractured bone, is a more difficult model for bone repair than other models, i.e., drilling, since the loose connective tissue that fills the defect gap is rich in fibroblasts, and releasing cytokines decrease the osteogenesis [66], that can be an explanation for the cartilage callus formation in the defect site.

Based on the results depicted in Figs. 3 and 7, although the amount of callus and new bone formation in all treated rats were close to each other, the quality of bone and the ability to tolerate external load were greater in the WBV group than in the other groups. This can be due to the fact that the load-bearing ability of bone is affected by a number of factors, including its volume fraction, microstructure and architecture, and degree of mineralization [67]. Another explanation for the greater impact of WBV than LLLT on the mechanical strength of the bone might be due to the different effects of these two stimuli. The low-level laser therapy can stimulate bone formation and accelerate fracture healing, but can likely not have a constructive effect on the bone microstructure, as the architecture and microstructural pattern of the newly formed bone can be likely better controlled through a mechanical stimulus, based on Wolff's law and bone remodeling theories [68–71]. In regard to the combined group (LV), their combination had no constructive and positive effects and it seems that they apparently had destructive interference on each other. In the LV groups, the amount of newly

formed bone was less than that in the LLLT group, and the maximum force to failure was less than that in the WBV group (see Figs. 4, 5, and 6).

The experimental model in the present study was found to be reproducible and easy to perform. The internal fixation allowed the rats to use their legs soon after surgery. The extent of initial trauma and the shape and site of fracture were well controlled, and the type of fixation used in this study enabled the micromovements needed for good fracture healing [5].

A limitation of this study was the use of only one frequency, one direction of vibration (however rats were free to move in their cells), and one amplitude. The LAHF vibration used in this study was selected according to the results of previous studies that demonstrated positive effects on human or rats' bone [24, 60, 72], and the intensity and laser source were selected according to optimization and modification in recent studies [18, 48, 73].

In conclusion, this study showed that both low-level laser therapy and low-amplitude high-frequency whole body vibration have a positive impact on the rate of bone healing in the fractured femur of rats fixed by a metal implant. It was also observed that low-level laser therapy had positive effects in the early stage of osteogenesis, as well as on the biomechanical properties of new bone formation, and LAHF whole body vibration had a stronger impact on the mechanical properties of healed bone compared to the LLLT method. Moreover, using LLLT and WBV simultaneously did not show constructive results compared to either method. As with the other studies on biological tissue repair, this work needs to be extended by other researchers in order to shed more light on the fractured bone healing process.

**Acknowledgments** The authors would like to thank AR Karian, M Kouhestani, A Mehin, S Salehi, Baqiyatallah University of Medical Sciences, AmirKabir University of Technology, Material and Biomaterial Research Center, and the Iranian National Center for Laser Science and Technology for their support.

## References

1. Lirani-Galvao AP, Jorgetti V, da Silva OL (2006) Comparative study of how low-level laser therapy and low-intensity pulsed ultrasound affect bone repair in rats. *Photomed Laser Surg* 24:735–740
2. Pretel H, Lizarelli RFZ, Ramalho LTO (2007) Effect of low-level laser therapy on bone repair: histological study in rats. *Lasers Surg Med* 39:788–796
3. Gjelsvik A (1973) Bone remodeling and piezoelectricity. *J Biomech* 6:69–77
4. Franco G, Laraia I, Maciel A, Miguel N, Dos Santos G, Fabrega-Carvalho C, Pinto C, Pettian M, Cunha M (2013) Effects of chronic passive smoking on the regeneration of rat femoral defects filled with hydroxyapatite and stimulated by laser therapy. *Injury* 44:908–913



5. Luger E, Rochkind S, Wollman Y, Kogan G, Dekel S (1998) Effect of low-power laser irradiation on the mechanical properties of bone fracture healing in rats. *Lasers Surg Med* 22:97–102
6. Obradovic R, Kasic L, Mihailovic D, Ignjatovic N, Uskokovic D (2007) Comparative efficacy analysis of biomaterials and soft lasers in repair of bone defects. *J Oral Laser Appl* 7:161–166
7. Pinheiro A, Limeira A, Marzola C (2003) Effect of low level laser therapy on repair of bone defects grafted with inorganic bovine bone. *Braz Dent J* 14:177–181
8. Diniz J, Nicolau R, Ocarino N, Magalhaes F, Pereira R, Serakides R (2009) Effect of low-power gallium-aluminium-arsenium laser therapy (830 nm) in combination with bisphosphonate treatment on osteopenic bone structure: an experimental animal study. *Lasers Med Sci* 24:347–352
9. Lopes CB, Pacheco MTT, Silveira L Jr, Duarte J, Cangussu MCT, Pinheiro ALB (2007) The effect of the association of NIR laser therapy BMPs, and guided bone regeneration on tibial fracture treated with wire osteosynthesis: Raman spectroscopy study. *J Photochem Photobiol B Biol* 89:125–130
10. Pinheiro A, Jr FL, Gerbi M, Ramalho L, Marzola C, Ponzi E, Soares A, Carvalho L, Lima H, Goncalves T (2003) Effect of 830-nm laser light on the repair of bone defects grafted with inorganic bovine bone and decalcified cortical osseous membrane. *J Clin Laser Med Surg* 21:383–388
11. Nicolau R, Jorgetti V, Rigau J, Pacheco M, Reis L, Zangaro R (2003) Effect of low-power GaAlAs (660 nm) on bone structure, cell activity: an experimental animal study. *Lasers Med Sci* 18:89–94
12. Khadra M, Kasem N, Haanaes HR, Ellingsen JE, Lyngstadaas SP (2004) Enhancement of bone formation in rat calvarial bone defects using low-level laser therapy. *Oral Surg Oral Med Oral Pathol Oral Radiol Endod* 97:693–700
13. Gerbi M, Marques A, Ramalho L, Ponzi E, Carvalho C, Santos R, Oliveira P, Noia M, Pinheiro A (2008) Infrared laser light further improves bone healing when associated with bone morphogenetic proteins: an in vivo study in a rodent model. *Photomed Laser Surg* 26:55–60
14. Chung H, Dai T, Sharma SK, Huang Y-Y, Carroll JD, Hamblin MR (2012) The nuts and bolts of low-level laser (light) therapy. *Ann Biomed Eng* 40:516–533
15. Lam TS, Abergel RP, Meeker CA, Castel JC, Dwyer RM, Uitto J (1982) Laser stimulation of collagen synthesis in human skin fibroblast cultures. *Laser Life Sci* 1:61–77
16. Cruz DR, Kohara EK, Ribeiro MS, Wetter NU (2004) Effect of low intensity of laser therapy on the orthodontic movement velocity of human teeth: a preliminary study. *Lasers Surg Med* 35:117–120
17. Khadra M, Ronold H, Lyngstadaas S, Ellingsen J, Haanaes H (2004) Low-level laser therapy stimulates bone-implant interaction: an experimental study in rabbits. *Clin Oral Impl Res* 15:325–332
18. AbuElsaad N, Soory M, Gasalla L, Ragab L, Dunne S, Zalata K, Louca C (2009) Effect of soft laser and bioactive glass on bone regeneration in the treatment of bone defects (an experimental study). *Lasers Med Sci* 24:527–533
19. Nissan J, Assif D, Gross M, Yaffe A, Binderman I (2006) Effect of low intensity laser irradiation on surgically created bony defects in rats. *J Oral Rehabil* 33:619–624
20. Adel S, Ayad K, Shaheen A (2011) Effect of low level laser therapy on bone histomorphometry in rats. *Life Sci J* 8:372–378
21. Pereira C, Sallum E, Nociti F, Moreira R (2009) The effect of low-intensity laser therapy on bone healing around titanium implants: a histometric study in rabbits. *Int J Oral Maxillofac* 24:47–51
22. Maluf A, Maluf R, Brito C, Franca FM, de Brito RB Jr (2010) Mechanical evaluation of the influence of low-level laser therapy in secondary stability of implants in mice shinbone. *Lasers Med Sci* 25:693–698
23. Fritton S, McLeod K, Rubin C (2000) Quantifying the strain history of bone: spatial uniformity and self-similarity of low-magnitude strains. *J Biomech* 33:317–325
24. Garman R, Guadette G, Donahue L, Rubin C, Judex S (2007) Low-level accelerations applied in the absence of weight bearing can enhance trabecular bone formation. *J Orthop Res* 25:732–740
25. Judex S, Donahue L, Rubin C (2002) Genetic predisposition to osteoporosis is paralleled by an enhanced sensitivity to signals anabolic to the skeleton. *FASEB J* 16(10):1280–82
26. Garman R, Rubin C, Judex S (2002) The structural response of trabecular bone to low-level mechanical stimuli. Second Joint EMBS/BMES Conference, Houston, pp 456–457
27. Judex S, Boyd S, Qin Y, Turner S, Ye K, Muller R, Rubin C (2003) Adaptations of trabecular bone to low magnitude vibrations result in more uniform stress and strain under load. *Ann Biomed Eng* 31: 12–20
28. Rubin C, Turner A, Bain S, Mallinckrodt C, McLeod K (2001) Anabolism: low mechanical signals strengthen long bones. *Nature* 412:603–604
29. Xie L, Jacobson J, Choi E, Busa B, Donahue L, Miller L, Rubin C, Judex S (2006) Low-level mechanical vibrations can influence bone resorption and bone formation in the growing skeleton. *Bone* 39:1059–1066
30. Gilsanz V, Wren T, Sanchez M, Dorey F, Judex S, Rubin C (2006) Low-level, high-frequency mechanical signals enhance musculoskeletal development of young women with low BMD. *J Bone Miner Res* 21:1464–1474
31. Rubin C, Pecker R, Cullen D, Ryaby J, McCabe J, McLeod K (2004) Prevention of postmenopausal bone loss by a low-magnitude, high-frequency mechanical stimuli: a clinical trial assessing compliance, efficacy, and safety. *J Bone Miner Res* 19:343–351
32. Ward K, Alsop C, Caulton J, Rubin C, Adams J, Moghul Z (2004) Low magnitude mechanical loading is osteogenic in children with disabling conditions. *J Bone Miner Res* 19:360–369
33. Rubin C, Pope M, Fritton JC, Magnusson M, Hansson T, McLeod K (2003) Transmissibility of 15-hertz to 35-hertz vibrations to the human hip and lumbar spine: determining the physiologic feasibility of delivering low-level anabolic mechanical stimuli to skeletal regions at greatest risk of fracture because of osteoporosis. *Spine* 28:2621–2627
34. Daly R (2007) The effect of exercise on bone mass and structural geometry during growth. *Med Sport Sci* 51:33–49
35. Judex S, Lei X, Han D, Rubin C (2007) Low-magnitude mechanical signals that stimulate bone formation in the ovariectomized rat are dependent on the applied frequency but not on the strain magnitude. *J Biomech* 40:1333–1339
36. Garman R, Rubin C, Judex S (2007) Small oscillatory accelerations, independent of matrix deformations, increase osteoblast activity and enhance bone morphology. *PLoS One* 2(7):e653
37. Ozcivici E, Garman R, Judex S (2007) High-frequency oscillatory motions enhance the simulated mechanical properties of nonweight bearing trabecular bone. *J Biomech* 40:3404–3411
38. Hwang S, Lublinsky S, Seo Y, Kim I, Judex S (2009) Extremely small-magnitude accelerations enhance bone regeneration. *Clin Orthop Relat Res* 467:1083–1091
39. Van-Pelt LF (1977) Ketamine and xylazine for surgical anesthesia in rats. *J Am Vet Med Assoc* 171:842–844
40. Sebben JE (1983) Surgical antiseptics. *J Am Acad Dermatol* 9:759–765
41. Madsen J, Hukkhanen M (1996) Fracture healing and callus innervations after peripheral nerve resection in rats. *Clin Orthop Relat Res* 353:230–240
42. Leppänen O, Sievänen H, Jokihaara J, Pajamäki I, Järvinen TL (2006) Three-point bending of rat femur in the mediolateral direction: introduction and validation of a novel biomechanical testing protocol. *J Bone Miner Res* 21:1231–1237

43. Callis G, Sterchi D (1998) Decalcification of bone: literature review and practical study of various decalcifying agents. Methods, and their effects on bone histology. *J Histotechnol* 21:49–58
44. Takagi K, Urist M (1982) The reaction of the dura to bone morphogenetic protein. *Ann Surg* 196:100–109
45. Ferreira G, Cestari T, Granjeiro J, Taga R (2004) Lack of repair of rat skull critical size defect treated with bovine morphometric protein bound to microgranular bioabsorbable hydroxyapatite. *Braz Dent J* 15:175–180
46. Marins L, Cestari T, Sottovia A, Granjeiro J, Taga R (2004) Radiographic and histological study of perennial bone defect repair in rat calvaria after treatment with blocks of porous bovine organic graft material. *J Appl Oral Sci* 12:62–69
47. Guehenec LL, Goyenville E, Aguado E, Houchmand-Cuny M, Enkel B, Pilet P, Daculsi G, Layrolle P (2005) Small-animal models for testing macroporous ceramic bone substitutes. *J Biomed Mater Res Part B Appl Biomater* 72:69–78
48. Silva-Jounior A, Pinheiro A, Oliveira M, Weismann R, Ramalho L, Nicolau R (2002) Computerized morphometric assessment of the effect of low-level laser therapy on bone repair: an experimental animal study. *J Clin Laser Med Surg* 20:83–87
49. Shakouri S, Soleimanpour J, Salekzamani Y, Oskuie M (2010) Effect of low-level laser therapy on the fracture healing process. *Lasers Med Sci* 25:73–77
50. Liu X, Lyon R, Meier H, Thometz J, Haworth S (2007) Effect of lower-level laser therapy on rabbit tibial fracture. *Photomed Laser Surg* 25:487–494
51. Zivcovic R, Kesic L, Mihailovic D, Ignjatovic N, Uskokovic D (2006) Investigation of HeNe laser therapy influence on BCP/PLGA osseointegration—experimental study. *Med Biol* 13:109–113
52. Queiroga A, Sousa F, Araujo J, Santos S, Sousa CF, Quintans T, Almeida T, Nonaka C, Batista L, Junior FL (2008) Evaluation of bone repair in the femur of rats submitted to laser therapy in different wavelengths: an image segmentation method of analysis. *Laser Phys* 18:1087–1091
53. Renno ACM, Moura FMD, Santos NSAD, Tirico RP, Bossini PS, Parizotto NA (2006) Effects of 830-nm laser light on preventing bone loss after ovariectomy. *Photomed Laser Ther* 24:642–645
54. Barbosa D, Villaverde AGJB, LoschiavoArisawa EA, Souza RA (2014) Laser therapy in bone repair in rats: analysis of bone optical density. *Acta Ortop Bras* 22:71–74
55. de Oliveira AM, Castro-Silva II, de Oliveira Fernandes GV, Melo BR, Alves ATNN, Silva Júnior A, Lima ICB, Granjeiro JM (2014) Effectiveness and acceleration of bone repair in critical-sized rat calvarial defects using low-level laser therapy. *Lasers Surg Med* 46:61–67
56. Weber JBB, Pinheiro ALB, Oliveira MG, Oliveira FAM, Ramalho LMP (2006) Laser therapy improves healing of bone defects submitted to autologous bone graft. *Photomed Laser Surg* 24:38–44
57. Kim Y-D, Kim S-S, Hwang D-S, Kim S-G, Kwon Y-H, Shin S-H, Kim U-K, Kim J-R, Chung I-K (2007) Effect of low-level laser treatment after installation of dental titanium implant-immunohistochemical study of RANKL, RANK, OPG: an experimental study in rats. *Lasers Surg Med* 39:441–450
58. Maia LGM, Alves AVF, Bastos TS, Moromizato LS, Lima-Verde IB, Ribeiro MAG, Júnior LGG, de Albuquerque-Júnior RLC (2014) Histological analysis of the periodontal ligament and alveolar bone during dental movement in diabetic rats subjected to low-level laser therapy. *J Photochem Photobiol B Biol* 135:65–74
59. Batista JD, Sargenti-Neto S, Dechichi P, Rocha FS, Pagnoncelli RM (2015) Low-level laser therapy on bone repair: is there any effect outside the irradiated field? *Lasers Med Sci* 30:1569–1574
60. Rubin C, Judex S, Qin Y-X (2006) Low-level mechanical signals and their potential as a non-pharmacological intervention for osteoporosis. *Age Ageing* 35:ii32–ii36
61. Leung KS, Shi HF, Cheung WH, Qin L, Ng WK, Tam KF, Tang N (2009) Low-magnitude high-frequency vibration accelerates callus formation, mineralization, and fracture healing in rats. *J Orthop Res* 27:458–465
62. Fritton JC, Rubin CT, Qin Y-X, McLeod KJ (1997) Whole-body vibration in the skeleton: development of a resonance-based testing device. *Ann Biomed Eng* 25:831–839
63. de Oliveira ML, Bergamaschi CT, Silva OL, Nonaka KO, Wang CC, Carvalho AB, Jorgetti V, Campos RR, Lazaretti-Castro M (2010) Mechanical vibration preserves bone structure in rats treated with glucocorticoids. *Bone* 46:1516–1521
64. Trelles M, Mayoyo E (1987) Bone fracture consolidates faster with low power lasers. *Lasers Surg Med* 7:36–45
65. Barushka O, Yaakobi T, Oron U (1995) Effect of low energy laser (HeNe) irradiation on the process of bone repair in the rat tibia. *Bone* 16:47–55
66. Granjeiro J, Oliveira R, Bustos-Valenzuela J, Sogayar M, Taga R (2005) Bone morphogenetic proteins: from structure to clinical use. *Braz J Med Biol Res* 38:1463–1473
67. Martin RB, Burr DB, Sharkey NA (1998) Skeletal biology. In: Martin RG, Burr DB, Sharkey NA (eds) *Skeletal tissue mechanics*. Springer, New York, pp 29–78
68. Wolff J, Wessinghage D. *Das gesetz der transformation der knochen: Schattauer*
69. Huiskes R, Ruimerman R, Van Lenthe GH, Janssen JD (2000) Effects of mechanical forces on maintenance and adaptation of form in trabecular bone. *Nature* 405:704–706
70. Rouhi G, Vahdati A, Li X, Sudak L (2015) A three-dimensional computer model to simulate spongy bone remodeling under overload using a semi-mechanistic bone remodeling theory. *J Mech Med Biol* 15:1550061
71. Vahdati A, Rouhi G (2009) A model for mechanical adaptation of trabecular bone incorporating cellular accommodation and effects of microdamage and disuse. *Mech Res Commun* 36:284–293
72. Judex S, Gupta S, Rubin C (2009) Regulation of mechanical signals in bone. *Orthod Craniofac Res* 12:94–104
73. Hubler R, Blando E, Gaiao L, Kreisner P, Post L, Xavier C, Oliveira M (2010) Effects of low-level laser therapy on bone formed after distraction osteogenesis. *Lasers Med Sci* 25:213–219